6-1-2016

# Assessment of DAF-19 Related Behavioral Defects

Loraina A. Stinson
*Lawrence University*, loraina.a.stinson@lawrence.edu

**Assessment of DAF-19 Related Behavioral Defects**

Loraina Stinson
Lawrence University
2016

I hereby reaffirm the Lawrence University Honor Code

# Table of Contents

**Assessment of DAF-19 Related Behavioral Defects**

Abstract

The *daf-19* gene encodes the only RFX transcription factors in *C. elegans*, producing at least four related protein isoforms, one of which, DAF-19C, is responsible for ciliogenesis. Previous work by Senti and Swoboda (2008) demonstrated that adult worms deficient in all four DAF-19 proteins have extremely aberrant dwelling and roaming behavior on bacterial food. Most intriguingly, the addition of cDNA encoding the DAF-19C isoform restores cilia formation, but does not fully restore wild-type dwelling and roaming behavior. We are suggesting that additional neuron functions are needed to properly execute behaviors and these neuron functions require the activity of other DAF-19 isoforms. We have tested this hypothesis using both classic assays of roaming behavior and a newly developed assay that mimics a patchy food environment to further probe worm foraging behavior. We are assessing the behavior of worms lacking all isoforms of DAF-19 as well as those containing mutant alleles that affect only the larger isoforms of DAF-19 to determine whether these isoforms play a role in nervous system function and worm behavior.

*Keywords: C. elegans, daf-19*

## Introduction

### Neural Circuits, Sensation to Behavior

With the exception of sight and touch, human newborns arrive in the world with most senses well developed. Their taste buds are mature at 14 weeks post-conception and their olfactory senses are mature by the end of the first trimester. Newborns then begin to develop their sense of touch. Touch and smell sensations are crucial for survival; they allow newborns to sense and recognize their mothers. These natural and basic sensations allow newborns to navigate through their universe. Later in life, touch sensation also leads to emotional, physical, and cognitive improvements in adults (Konnikova et al., 2016). Specialized cellular protrusions called cilia facilitate the understanding of all sensation. Cilia are responsible for the neural circuits that allow sensation to be processed and become behavior. Yet, not all cilia are the same.

Cilia are hair-like organelles that project from cell surfaces, made up of microtubules extending from the cell, still sharing the plasma membrane. Cilia have one of two possible functions: motile cilia, which move cells through liquids allow for cell motility, and non-motile cilia which are involved in multiple forms of sensation. Motile cilia exert mechanical force to create movement to project the cell through fluid, *i.e.* sperm swimming, or to move liquids past a cell, such as in the lungs. Non-motile cilia are sensory organelles that contain a variety of receptors; they can sense differences in the environment, including the presence of odorants, and changes in pH. Cilia facilitate sensory processes as well as membrane and protein transport inside the cell.

In humans, cilia are found in multiple organs, including the nose, eyes, and lungs. They are key players in numerous physiological, developmental, and sensory processes such as

hearing, olfaction, and photoreception (Falk et al., 2016). The cilia in our ears are stereocilia which are mechanosensing organelles of hair cells that respond to fluid motion. Our color vision does not rely on cilia but our night vision, controlled by rods, contain disk membranes that have cilia on them (Gilliam et al., 2012).

In the human olfactory system, sensation transduction is the conversion of a sensory stimulus into a signal through the nervous system that results in a behavioral response. The informational process occurs in the olfactory epithelium, composed of a blanket of neurons, and basal and structural sustentacular cells that cover about half of the nasal cavity. Receptor neurons receive olfactory information by the cilia that extend out from their cell bodies into a layer of mucus (Purves et al., 2001). An odorant will begin a signal transduction cascade by binding to a ligand-gated metabotropic channel (ion channels on the plasma membrane controlled by signaling mechanisms) within the ciliary membrane. An odorant binding usually activates a channel opening to induce an influx of sodium or calcium into the neurons, generating an electronic signal that is passed particularly to interneurons either via gap junctions or neurotransmitter release. These interneurons reach the brain where sensory signals are sent out to the motor system to effect behavior. Recent studies have shown that despite the weak representation of olfactory receptors common in other species, the cortical areas of integration of olfactory sensations in humans are very large and have important interconnections with memory, language, and neuro–vegetative areas (Sarafoleanu et al., 2009). This is the reason we have memories associated with distinct smells or why we turn our heads towards the popcorn machine at the movie theaters. Subconscious human behaviors are a result of sensory stimuli coming in from the environment, being received by cilia on sensory neurons, being transduced into

neuronal activity, and traveling back out to the extremities to elicit a behavior through our motor neurons.

Genetic defects in ciliary proteins responsible for cilia formation, maintenance, or function result in a variety of human diseases such as anosmia (the loss of the sense of smell), and retinal degeneration. Evidence indicates that ciliary defects can lead to an even broader set of both developmental and matured attributes, with mutations in ciliary proteins now associated with nephronophthisis (impaired kidney function), Bardet-Biedl syndrome (a genetic disorder characterized by obesity, retinitis pigmentosa, polydactyly, hypogonadism, and renal failure), and Alstrom syndrome (a rare genetic disorder characterized by multiorgan disorder). Recently, ciliary defects have been observed in neurodegenerative diseases, such as Huntington's disease (a condition in which nerve cells break down over time). Studies reveal the degeneration of neurons may lead to, or advance, symptoms of neurodegenerative diseases (Liu et al., 2011). Since the molecular pathways mediating ciliary functions are evolutionarily conserved within the animal lineage, studying neuronal maintenance in other organisms, such as *C. elegans*, will help us systematically understand how neurons communicate with each other and how their functions are maintained during aging.

### *C. elegans*

*Caenorhabditis elegans* are non-parasitic, transparent nematodes introduced as model organisms for developmental biology and neurobiology by Sydney Brenner in 1963 (Inglis et al., 2007). Even though the *C. elegans* genome is about 30 times smaller than the human genome, it codes for 22,000 proteins, which is only slightly fewer than that encoded by the human genome. About 35% of *C. elegans* genes and proteins are closely related to human genes and proteins

(Mitreva et al., 2014). Since their introduction, *C. elegans* have been used in a multitude of studies that have earned Nobel Prizes, several of which are relevant to the study described here. From 1976 through 1980, a complete cell lineage of *C. elegans* was published by John Sulston and colleagues. In 1994, Martin Chalfie et al. used *C. elegans* to discover how to tag genes with green fluorescent protein, a technique that allows us to identify single neurons in living worms (Chalfie et al., 1994). A complete map of their genome, including the neuronal cell lineage of *C. elegans* neuronal connections was published by John White in 1998.

*C. elegans* develop from a fertilized egg that divides to form into a 959 somatic celled hermaphrodite or a 1031 celled male. A full wild-type adult is 1mm in length with an outer body cavity consisting of the cuticle, hypodermis, excretory system, neurons, and muscles (Fig.1).

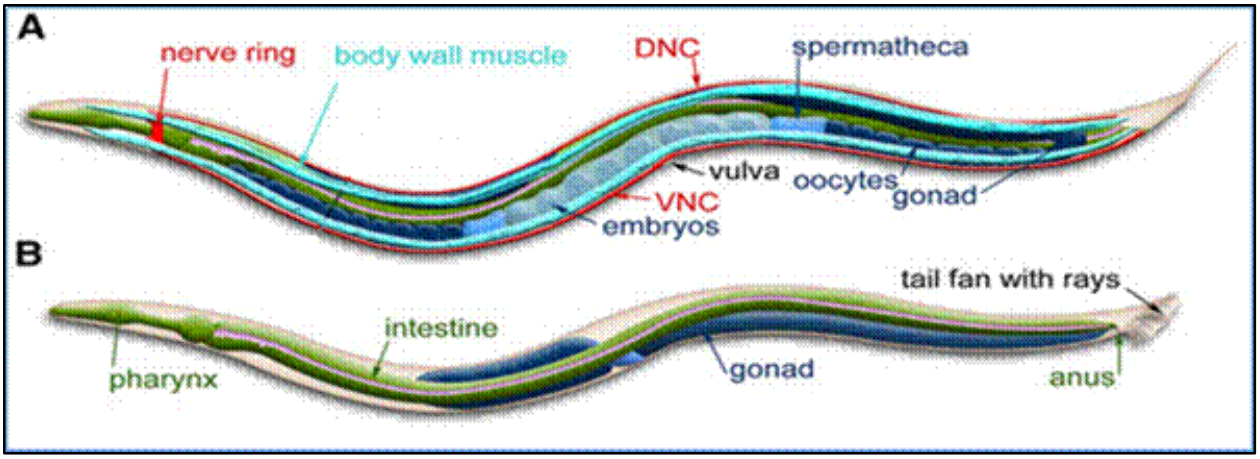


**Figure 1: *C. elegans* anatomy.** Lateral views of hermaphrodite (A) and male (B) worms. (A) The dorsal nerve cord (DNC) and ventral nerve cord (VNC) run along the length of the animal starting at the nerve ring. (B) The inner body cavity contains the pharynx, intestine and gonads. The nervous system and muscles are omitted in this view. Images modified from those found at www.wormatlas.org (Altun et al., 2009).

The inner body cavity contains the pharynx, intestine, and gonads. Neural structures include sensory organs in the head which mediate responses to taste, smell, temperature, and touch, excluding sight (Inglis et al., 2005).

*C. elegans* have two sexes, hermaphrodite or male, which are determined by the ratio of X chromosomes to autosomes. Male *C. elegans* are formed by spontaneous non-disjunction in the hermaphrodite germ line but have a higher chance of being produced by matings with a male, or following heat-shock of a young hermaphrodite. A physical difference between an adult male and adult hermaphrodite is that the male's reproductive system starts to develop at the L2 stage and the morphology of the male tail is characterized by a "hook" and fan structure. The hook is used to sense and impregnate the hermaphrodites (Lints et al., 2005). Hermaphrodite *C. elegans* are a self-sustaining sex that uses internal self-fertilization to create progeny. A wild-type hermaphrodite worm can produce up to 300 progenies alone, and even more when mated with a male.

In the laboratory, populations of *C. elegans* are easily maintained on an agar plate seeded with lawns of *Escherichia coli* OP50 incubated at 20 ℃. Their short generation time of 3 days yields simple maintenance and upkeep of populations. The full life cycle lasts up to three weeks. When conditions are not optimal, L1 larvae worms can enter the dauer life stage; this is marked by a metabolic shift regulated by a series of hormonal signaling pathways that allows them to temporarily exit the life cycle. This survival mechanism allows *C. elegans* to survive when population density is high and food supply is low. Once living conditions improve, animals continue development at the L4 larval stage (Wolkow et al., 2016).

Clearly, one of the most interesting traits about *C. elegans* is their transparency. It allows a unique advantage when studying the organism because their entire anatomy is easily viewed with light microscopy allowing researchers to follow cell lineages, distinguish larval stages, as well as identify fluorescent tags and dyed neurons. *C. elegans* have become models for genetics, molecular, developmental and cell biology, neurobiology, and behavior. They have various

mechanical behavioral response. Some are initiated by touch, while others, like male mating behaviors, are more natural. Other behaviors are sensory responses, such as osmotic avoidance (Hart, 2006).

## *C. elegans* Neurobiology

*C. elegans* are used to advance knowledge about human neurobiology. They are currently being used as models to study various neurodegenerative diseases (Dimitriadi and Hart, 2010). In hermaphroditic *C. elegans*, 60 ciliated sensory neurons provide the ability to sense physical and chemical environments. Most of their nervous system is located in the head of the animal (Boulin, 2001). There are various types of neurons, but each neuron is composed of the same four regions:  the dendrites, the cell body, the axons, and the axon terminals. The dendrites are long, thin branches from the cell body which are the source of connections through nerve impulses of adjoining neurons (Fig.2). Information flows from the dendrites to the cell body to the axon. The cell body contains the nucleus and is also the site of protein and membrane synthesis. The axons are nerve fibers that extend from the cell body, terminating with synaptic knobs that send nerve impulses or neurotransmitters out to downstream neurons (dendrites) or muscle cells.

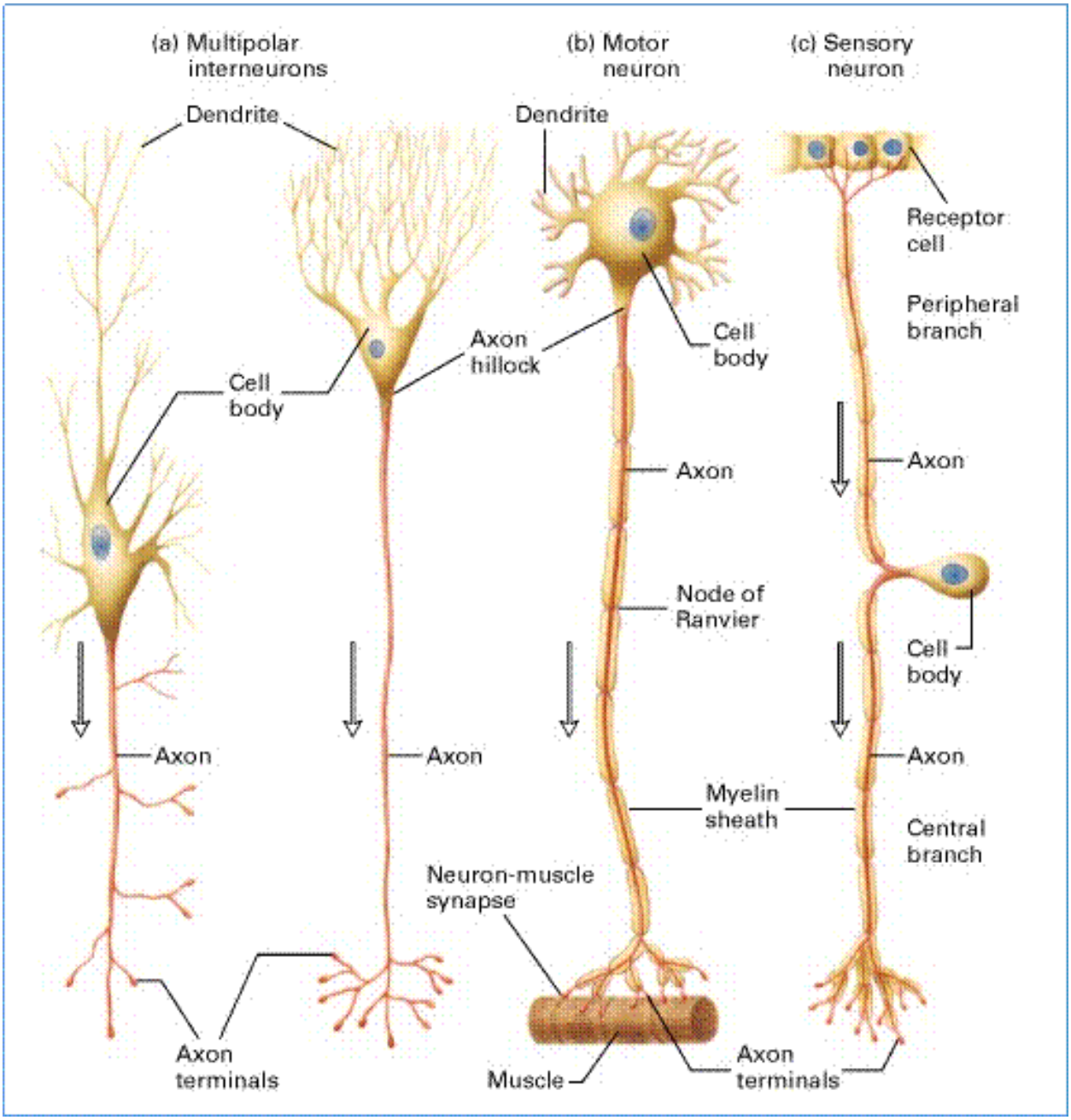


**Figure 2: Structures of typical mammalian neurons.** The cell bodies, dendrites, axons, and axon terminals are labeled for (A) multipolar interneurons, (B) motor neurons, and (C) sensory neurons. Arrows indicate the direction of conduction of nerve impulses in axons. (Image modified from Lodish et al., 2000)

*C. elegans'* neurons lack myelination, nodes of Ranvier, and receptor cells, but otherwise share the morphologies above. Though *C. elegans* lack what we usually call a brain, neuron cell

bodies are collected in several ganglia (see Fig. 3) where axons and dendrites of different neurons can be in close proximity and signals can be passed from sensory neurons to interneurons to motor neurons, thereby eliciting a behavioral response. There are two large groups of sensory receptors, called amphids (see Fig. 3), which are considered to be the main chemosensory organs because several nerve endings (dendrites) are exposed to the external environment (Boulin, 2001).

Adult hermaphrodites have 302 neurons, 60 of which are non-motile ciliated sensory neurons. Dendrites, the end of which can be ciliated, extend to the anterior end of the worm. *C. elegans* have six neurons that surround the mouth; these neurons have shorter cilia that are exposed to the external environment through openings in the cuticle. Ciliated neurons have also been identified in the tail of the organism and by the anus.

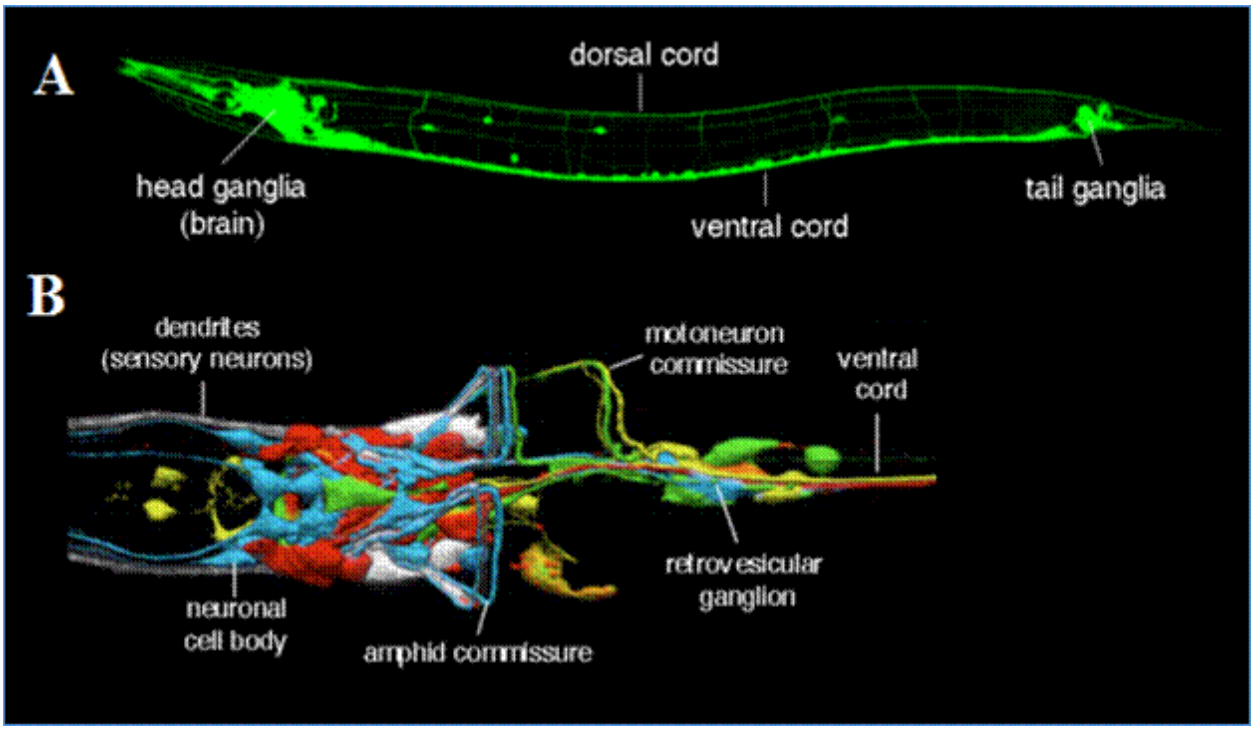


**Figure 3: Central Nervous System of *C. elegans*.** (A) All neurons labeled with GFP fluorescent marker. Head and tail ganglia are indicated. (B) A schematic of the neurons on the head region

of a *C. elegans.* Image modified from Hutter (2008). The main chemosensory organs of *C. elegans* are formed from a collection of amphid neurons. The cell bodies are located in the anterior region of the anterior pharyngeal bulb. The male neuroanatomy contains 170 neurons (81 male-specific and 89 shared neurons) and 64 muscles (Chklovskii and Bargmann, 2012). Male *C. elegans* have additional ciliated sensory neurons, most of which are found in the male tail. These sensory neurons guide male behavior in reaching and fertilizing oocytes (Inglis et al., 2007).

Some ciliated neurons are specialized morphologically and functionally to detect mechanosensation. Modified cilia at dendrite endings serve as sites of sensory signal capture and transduction. Chalfie et al. (1985) analyzed the neural pathway responsible for the touch circuit in *C. elegans.* Touch-induced movement is built from the six touch receptors, five pairs of interneurons, and 69 motor neurons. They determined the functions of these cells in the nervous system by laser ablation, demonstrating that there are two pathways for touch-mediated movements for anterior touch and only one for posterior touch. They also demonstrated that there is overlap in the neurons responsible for touch-mediated movement. Ciliated neurons are responsible for sensation, creating the possibility that ciliated neurons may also affect the motor functions of *C. elegans.* Furthermore, the ciliary mutants like *che-13* show significantly reduced abilities to respond to a touch on the nose of the animal (Kaplan and Horvitz, 1993). Further research from Hart et al. (1995) and Kaplan and Horvitz (1993), suggests that cilia may have a touch of influence in the mechanosensory role.

Like most neurons in *C. elegans,* the touch cells have a simple structure. Each cell has a single long receptor process that extends anteriorly from the cell body and lies next to the cuticle. This explains the touch-induced movements that Chalfie et al. (1985) demonstrated. When a worm is gently prodded by the head, it will move backwards, when it is prodded by the tail it will move forwards. It is possible to divide the cells into an anterior set and a posterior set by the response they produce (Chalfie et al., 1985). Movement in *C. elegans* results from the alternate

contraction and relaxation of the dorsal and ventral body wall muscles. A miscommunication in the motor neurons would alter or omit behavioral responses.

**The Roles of DAF-19**

In worms and humans, proteins function as catalysts, transporter molecules, and mechanical support. They also control growth and differentiation (Berg et al., 2002). Transcription factors (TF) are a class of proteins that bind to DNA so that transcription is affected, changing the expression of a gene or multiple genes. For example, the Regulatory Factor X gene family (RFX) encodes transcription factors in humans and other animals. RFX encodes a TF that has been found to modulate ciliary gene expression. Mutations in RFX genes lead to devastating human ciliopathies. RFX3 in mammals is crucial for proper cilia development in embryo nodal cells, brain ependymal cells, and pancreatic cells (Chu et al., 2011).

There are seven known RFX proteins in humans, though only one has been found in *C. elegans* (Aftab et al., 2008). Dubruille et al., (2002) demonstrated that in *Drosophila*, an RFX transcription factor is an essential regulator of ciliated sensory neuron differentiation. RFX mutant flies show defects in chemosensory and mechanosensory behaviors. The mutant behavioral phenotypes are correlated with abnormal function and structure of neuronal cilia, as shown by the loss of sensory transduction and by defects in ciliary morphology. This is consistent with RFX expression in ciliated sensory neurons and neuronal precursors (Dubruille et al., 2002).

The RFX human homologue transcription factor, DAF-19, in *C. elegans* has allowed scientists to study RFX TF functions *in vivo*. The *daf-19* gene was discovered during studies of

the dauer stage of development of *C. elegans*. *daf-19* null mutant worms constitutively enter the dauer stage even if environmental conditions are optimal for continued development. These mutants also lack normal dye-filling (a simple method that allows researchers to assay the structural integrity of sensory cilia by testing the ability of worms to take up a fluorescent dye (Inglis et al., 2007)) in their neurons and are highly defective in taste or smell. Swoboda et al. (2000) discovered that the *daf-19* gene is expressed specifically in all ciliated sensory neurons and that *daf-19* loss-of-function mutants cause the absence of cilia, resulting in sensory defects. Swoboda also attempted to identify the target control region where DAF-19 protein binds in order to activate genes that drive cilia development. This research demonstrated that some genes that function in all ciliated sensory neurons have RFX target sites, DNA sequences called x-boxes, and they require *daf-19* function for their activation. However, other genes responsible for the development of ciliated sensory neurons do not have those target sites and are not *daf-19* dependent (Swoboda et al., 2000).

Multiple products of the *daf-19* gene have been discovered by Senti and Swoboda (2008). Two longer protein isoforms, DAF-19A and DAF-19B, that differ only by the inclusion exon 4, are expressed in non-ciliated neurons while the short isoform, DAF-19C, is expressed in ciliated neurons (Fig. 4). DAF-19M was discovered by Wang et al. (2010) as an isoform required for cilia specification in particular male-specific neurons. That is, the DAF-19M isoform determines what sensation the cilium should ‘perceive’ and thus transmit to downstream neurons.

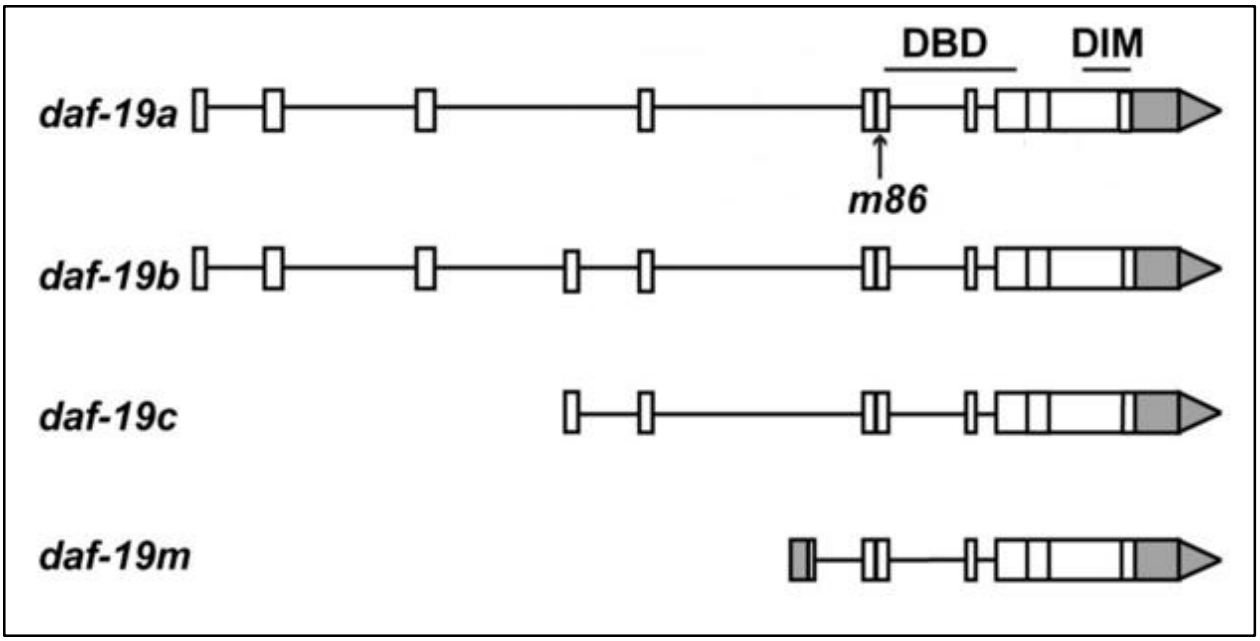


**Figure 4: Isoforms of *daf-19*.** Boxes depict exons on the horizontal line depicting introns. The *m86* stop codon location is indicated on isoform a, but affects production of all DAF-19 isoforms. Every isoform has the same DNA binding domain (DBD) and dimerization domain (DIM). Image adapted from Wang et al. (2010).

These isoforms confer starkly different behavioral phenotypes. Senti and Swoboda (2008) demonstrated that adult worms deficient in all four DAF-19 proteins have extremely aberrant dwelling and roaming behavior on food. The addition of cDNA encoding the DAF-19C isoform restored cilia formation, but did not fully restore dwelling and roaming behavior. "Dwelling" is the time a worm spends in one location feeding, usually where the *E. coli* is the thickest and perhaps has the highest oxygen levels (near the edge of the bacterial lawn). "Roaming" is when a worm is moving around the plate of food in search of new, untouched *E. coli.* These behaviors may also be interrupted when a hermaphrodite worm is about to lay eggs or when a worm is molting into a new life stage and enters a lethargus or a "sleep-like stage" (Raizen et al., 2008).

In 2000, Swoboda found that DAF-19 regulates the expression of genes required for the structure and function of cilia in *C. elegans*. In 2008, Senti and Swoboda speculated that DAF-19A/B maintains synaptic protein expression in non-ciliated neurons through an indirect mechanism. They found that the short isoform, DAF-19C, is specifically expressed in ciliated sensory neurons and expression of it alone can rescue all cilia-related phenotypes of *daf-19* mutants. In contrast, the long isoforms DAF-19A/B are expressed from a different promoter, and are expressed in almost all non-ciliated neurons. It is believed that the different DAF-19 isoforms activate different target genes through an x-box or related DNA sequences. Senti and Swoboda (2008) also observed the reduction of several synaptic proteins after the loss of *daf-19*, a phenotype which is rescued by the addition of DAF-19 A/B isoforms (Fig. 5).

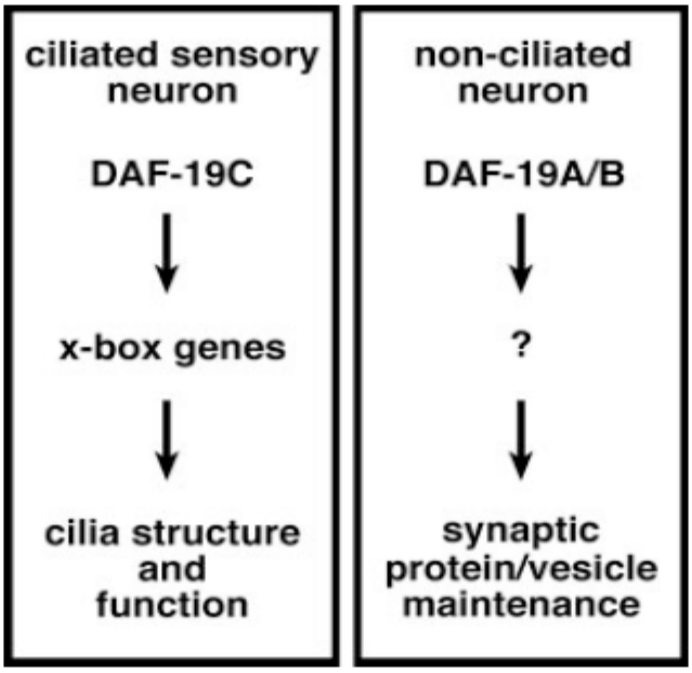


**Figure 5: DAF-19 isoform functions.** DAF-19C controls cilia structure and function by regulating expression of x-box genes. DAF-19 A/B controls synaptic protein/vesicle maintenance through an unknown pathway (Senti and Swoboda, 2008).

The use of wild-type *C. elegans* circuitry allows for a defined model of how neurons function together to generate behavior. Wild-type worms will dwell on the edge of the *E. coli* then roam around the food and dwell in new areas around the *E. coli* spot (Fig. 6B). On the other spectrum of behaviors, *daf-19(m86)* mutants only move a small distance, rarely reaching the edge of the plate (Fig. 6D). When adding back the *daf-19c* construct to *daf-19(m86)*, only dwelling behavior is restored (Fig. 6F). When expressing *daf-19a* alone, only roaming behavior is expressed aberrantly (Fig. 6G) . These behavioral phenotypes suggest that the different *daf-19* isoforms have different functions related to sensation circuitry.

To test whether the lack of synaptic proteins were a fault in the pre- or postsynaptic vesicles, Senti and Swoboda (2008) tested resistance to the paralyzing effects of pharmacological substances aldicarb (acetylcholinesterase inhibitor) and levamisole (nicotinic anthelmintic drug), and they also discovered that *daf-19* mutants that were resistant to the paralyzing effects, showed to have reduced synaptic vesicle proteins (Mahoney et al., 2006; Qian et al., 2008). In addition, the lack of all DAF-19 isoforms results in impaired dwelling/roaming behavior of the worm. These behavioral phenotypes can be rescued by the long isoform DAF-19A and DAF-19C, but not by DAF-19A alone.

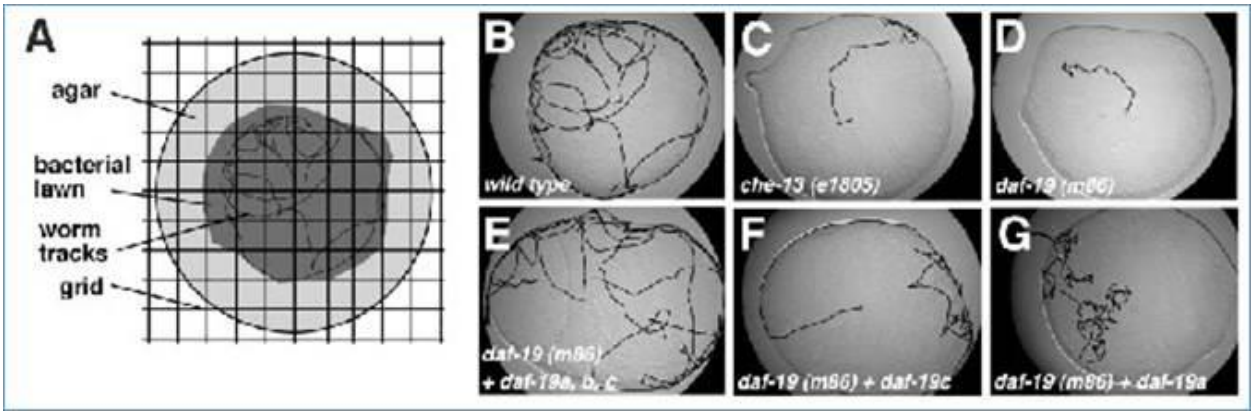


**Figure 6: Behavioral Defects of *daf-19* Mutant Worms.** A dwelling and roaming assay is used to assess whether DAF-19A and DAF-19C are required for complete rescue of the dwelling/roaming phenotype of *daf-19* mutants. (A) Schematic visualization of the method for analyzing the dwelling/roaming assay. (B) Wild-type worms dwell in high food concentrates and will roam to find newer food sources. (C) The negative control, *che-13* mutants, neither dwell nor roam. (D) *daf-19(m86)* missing all isoforms of DAF-19, roam and dwell even less. (E) By expressing all isoforms in *daf-19(m86),* wild-type behavior is restored. (F) When only expressing *daf-19c*, only dwelling behavior is restored. (G) When only expressing *daf-19a,* only roaming behavior is rescued. Assays were conducted by placing a single worm in the center of a 6mm agar plate seeded with OP50 *E.coli* and observing its behavior for an hour. Figure and legend modified from Senti and Swoboda (2008).

**Previous Studies on the Function of Daf-19A/B**

To understand the role of DAF-19 in neuronal processes other than ciliogenesis, De Stasio undertook a transcriptome analysis using populations of 2-day old adult worms, *daf-19 (m86)* and isogenic wild-type worms (De Stasio, unpublished). These worms would have completed ciliogenesis, thus she hoped to asses the role of *daf-19 A/B* isoforms in controlling gene expression. She assessed relative transcript levels of ~18,000 genes and found 700 that were differentially expressed in *daf-19(m86)* worms. Many students have characterized the expression pattern and *daf-19* dependence of over 30 of these genes using GFP transcriptional

fusion constructs. Thus far, ten new genes have been identified as *daf-19* target genes. These genes are regulated by DAF-19 exclusively in neurons.

## Current Study

We are characterizing new *daf-19* mutations that we predict should affect only specific *daf-19* isoforms in hopes to link a distinct behavioral phenotype to each isoform. In this way, we hope to narrow down the function of each isoform. In addition to performing dwelling and roaming assays, we developed a related assay that mimics a patchy food environment to further probe worm foraging behavior. We are testing worms lacking all isoforms of DAF-19 as well as those containing mutant alleles that affect only the larger isoforms of DAF-19 to determine whether these isoforms play a role in nervous system function and behavior.

## METHODS

### Strains and Culture Methods

All strains except *daf-19(m86)* were grown at 20°C. *daf-19(m86)* worms were kept at 15°C to allow for a low level of adult development. L4 worms were picked and placed on a fresh standard nematode growth medium (NGM) agar plate streaked with OP50 twelve to 24 hours prior to starting every assay. All strains were tested on the same day for each repetition of every assay.

### Dwelling Roaming Assay

Assays were done using freshly made and freshly streaked 5 cm NGM plates with a standard size bacterial lawn. One worm was placed in the middle of the OP50 E. coli lawn for one hour, then removed. The tracks were counted using a 5 mm x 5 mm transparent grid and the percent of the plate covered was enumerated. Assays were executed in a controlled environment with a constant temperature of 20°C.

**5-Spot Assay**

Assay plates were executed on 5 cm nematode growth medium agar plates seeded with five spots of 2ul of OP50 (at an A600 of 0.5) each. The 5-spot pattern was that seen on dice. Bacteria were left to grow at 20 ℃ for 36-48 hours prior to assay. One worm was placed in the middle of the center E. coli spot for an hour and then removed. Behavior was categorized by movement of single worm following tracks on the 5-spot food formation.

**Paralysis Assay**

Assays were performed on 5 cm NGM plates containing 500 µM aldicarb or 100 µM levamisole. 30 one day old adult worms were examined for each strain. Worms were classified as paralyzed when they did not move upon prodding with a pick three times in a row and were picked off the plate.

**DiI Staining**

Well-fed worms were transferred from a plate into 1 ml of m9 buffer in an 1.5 ml eppendorf tube. Then they were left 3-5 minutes to settle into a pellet. The supernatant was removed, leaving loose worm pellet. Worms were resuspended in 1 ml of M9 and add 5ul of DiI stock solution [1:100] and incubated in slow shaker for 1 hour. Worms were spun and washed with M9 before transferring them to NGM agar plates and then were allowed to crawl onto the OP50 bacterial lawn before viewing under microscope.

**Strain Constructions**

Two rescue strains were created by mating hermaphrodite L4 OE3198 *(daf-19m86 + A)* with male from *daf-19(of5)* and *daf-19(tm5562*) respectively. Genotype was confirmed by green coelomocytes marker (unc-122:: gfp) that was added to *daf-19(m86)* and positive dye-filling for three generations.

**Results**

In order to characterize the function of each isoform of DAF-19, we are trying to assign distinct behavioral phenotypes to worm strains containing isoform-specific mutations in the *daf-19* gene. We began by testing worm roaming ability in the dwelling and roaming assay. We then tested worm foraging behavior in a new related assay that mimics a patchy food environment.

This assay tests whether worms will leave a food source or stay put while the original assay tests how much worms will roam within a larger patch of food. It is possible that this latter assay will show us how the *daf-19* mutations affect ciliated sensory neurons. Lastly, we assessed worms for neuronal deficiencies by measuring their sensitivity to a pharmacological substance that causes excess activation of the neuromuscular junctions and hence leads to paralysis. We are testing all worms lacking all isoforms of DAF-19 as a control, as well as those containing mutant alleles that affect only the larger isoforms of DAF-19.

### ***daf-19*** **Mutant Isoforms**

*daf-19(of5)* is a CRISPR-CAS9-induced mutation (produced by Deborah Sugiaman) in which the original ATG translation start site of exon 1 is deleted. A total of 12 base pairs is removed but most importantly, this mutation creates a new ATG in the +1 reading frame, creating an in-frame stop codon in exon 2 after 29 amino acids are encoded. We thus expect this mutation to create a *daf-19* locus that does not express DAF-19A or B isoforms, but that does express DAF-19C. Because *daf-19(of5)* worms do dye-fill, we know that functioning cilia are produced, thus DAF-19C is apparently unaffected by the *of5* mutation.

*daf-19(of6)* is also a CRISPR-CAS9-induced mutation that includes a 53 base pair deletion at the 3' end of exon 4. This deletion removes the 3' splice site and creates a new stop codon at the end of the exon and the first base of the intron. The stop codon is at amino acid #159 in *daf-19B.* The *of6* allele was expected to affect production of DAF-19B and C isoforms, but should leave isoform A production unaffected. However, since *daf-19(of6)* worms also dye-fill, we assume that DAF-19C is produced. The allele may, however, fail to produce functional DAF-19B.

*daf-19(tm5562)* is a trimethylpsoralen-induced deletion from the Mitani Lab (unpublished). This 865 base pair deletion removes all of exon 2 (189 base pairs) and 583 base pairs of intron 1, and 93 base pairs of intron 2. This 865 base pair change results in the deletion of 63 amino acids. It appears that exon 1 and 3 could be spliced together and would maintain the original reading frame. *daf-19(tm5562)* worms were back-crossed five times with N2 wild-type worms by Savannah Vogel (Vogel, 2015) and Kristen Bischel (unpublished) in the De Stasio lab.

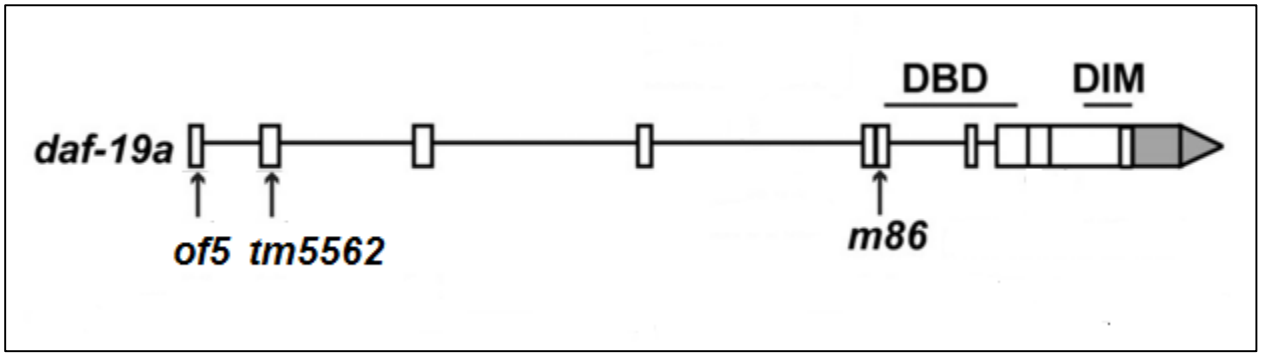


**Figure 7: Mutated Isoforms of *daf-19* including *of5* and *tm5562*.** Boxes depict exons on the horizontal line depicting introns. The *m86* stop codon location is indicated on isoform a. Every isoform has the same DNA binding domain (DBD) and dimerization domain (DIM). Image and legend adapted from Wang et al. (2010).

The behavior of worms from eight different strains were assayed in the present study. These worm strains included the following relevant genotypes: wild-type (N2), *daf-19(m86)* null mutant, *che-13(e1805), daf-19(tm5562), daf-19(of6), daf-19(of5)* and the *daf-19a* rescued strains; *daf-19(of5+a), daf-19(tm5562+a), daf-19(m86+a). che-13* worms lack ciliated sensory neurons and are used as a negative control in some behavioral assays along with *daf-19(m86).*

| Strains | Alleles | Affected Isoforms |
|---|---|---|
| N2 Wild-type | | |
| OE3063 | *daf-19(m86)* | All isoforms of DAF-19 missing |

| | | |
|---|---|---|
| CB3323 | *che-13(e1805)* | Dysfunctional ciliated sensory neurons |
| LU628 | *daf-19(tm5562)* | DAF-19A & B (2nd exon) |
| LU659 | *daf-19(of6)* | Thought to be a DAF-19 C mutation |
| LU632 | *daf-19(of5)* | DAF-19A & B null |
| LU673 | *daf-19(tm5562) + daf-19a* | Add DAF-19A to DAF-19A/B mutant |
| LU674 | *daf-19(of5) + daf-19a* | Add DAF-19A to DAF-19A/B null mutant |
| OE3198 | *daf-19(m86) + daf-19a* | Add DAF-19A to null background |

**Table 1: Assayed worms with corresponding alleles and affected isoforms.**

**Dwelling/Roaming Behavior**

The dwelling/roaming assay used by Senti and Swoboda (2008) is a method of quantifying defective behavioral phenotypes observed in *daf-19* mutants. In this assay, we quantify the percent of OP-50 covered by worm tracks in an hour period. A 5mm x 5mm grid is used to determine track coverage. The average wild-type worm dwells on the edge of the food patch where there is a higher concentration of bacteria and then roams to find newer bacterial food (Fig. 6B). Roaming behavior is quantified by the percent of 5X5mm grids containing worm tracks. We undertook replicate assays on eight dates with 30 worms per assay date. The frequency of total grids containing worm tracks relative to the number of grids containing *E. coli* was determined for each worm on each date. A two-way ANOVA using both strain and date as factors revealed that assay date was a significant factor *($p=0.00000393$),* thus we could not use each assay date as a replicate, but instead needed to analyze each date separately.

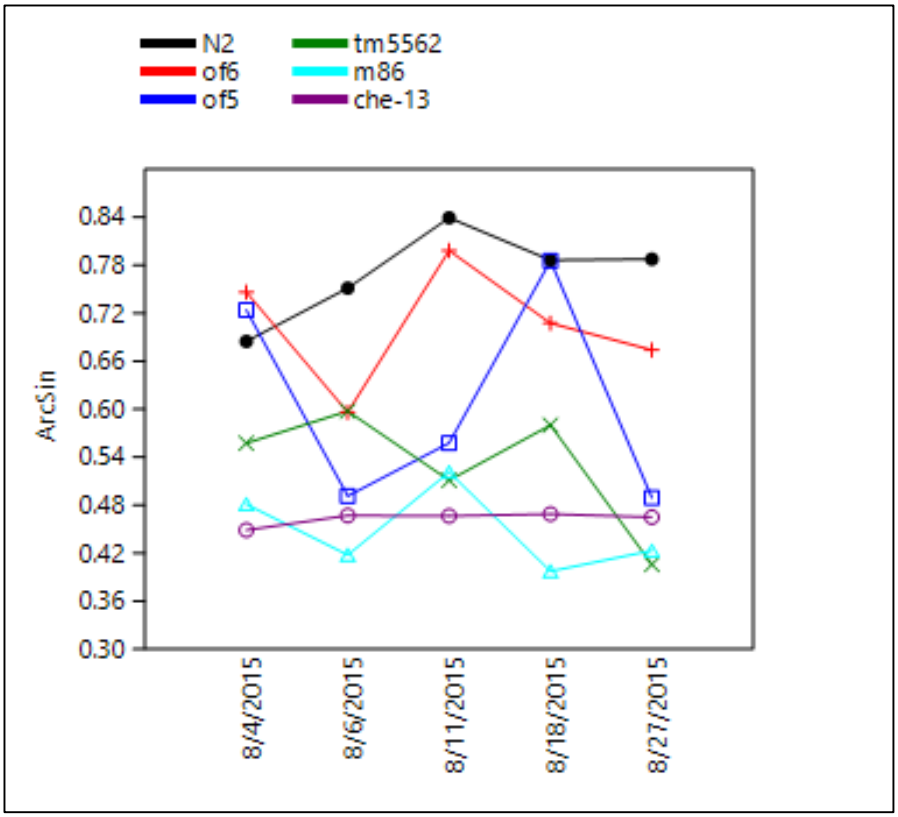


**Figure 8: Two-way ANOVA Graph-Date and Strain Interaction.** The p-values from the two-way ANOVA tests shows us significant differences among assay dates *(p=0.00000393),* and strains *(p=1.62E-68).*

Worm strain was also a significant factor in the two-way ANOVA *(p=1.62E-68).* One-way ANOVA tests revealed there were significant differences among strains for each date, thus we used Tukey's Pairwise Comparisons to identify which strains differed significantly in their roaming behavior. All dwelling and roaming results are reported as p-values from the pair-wise comparisons.

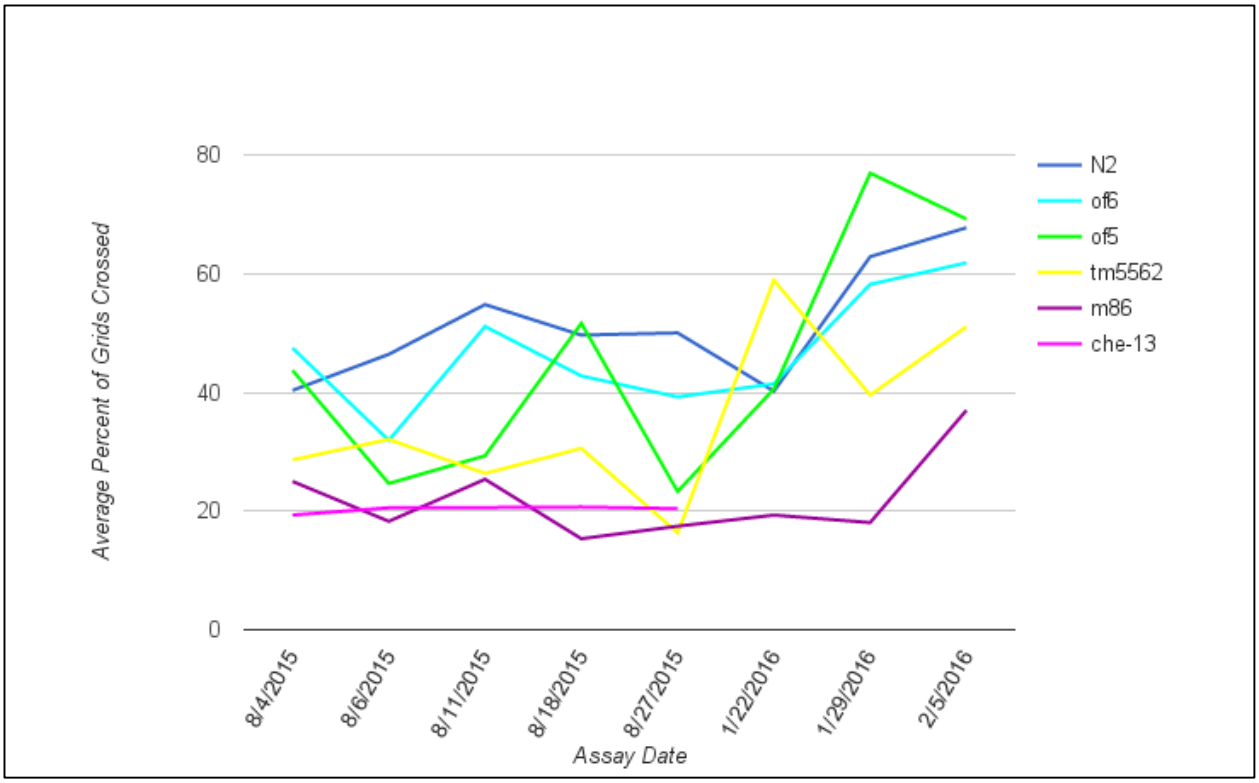


**Figure 9: Total Average Percent of Grids Crossed per Assay Date.** Quantification of the average grids crossed per date, raw data were arcsine transformed to correct for non-normality, then back transformed into percentages.

As expected, the mutant strains that either do not have cilia, *daf-19(m86),* or that lack functioning cilia, *che-13(e1805),* were not significantly different from each other on all five assay dates on which they were tested together (average $p=0.86276$). Their roaming behavior is very defective and the roaming range is limited.

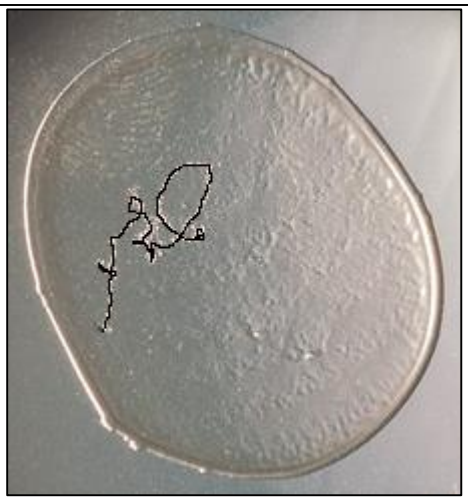

**Figure 10: Dwelling/Roaming Tracks of *che-13* Worms.** Visual representation of a single *che-13* worm after an hour on the food lawn. Image by Rachel Crowl.

The behavior of *che-13* worms was significantly different from that of N2 wild type worms on all five assay dates (average *p=0.0000218)*. The *che-13* worms roamed significantly less than N2 wild-type worms on all five assay dates and *daf-19(m86)* worms also roamed significantly less than N2 wild-type worms on all eight assay dates (average *p=0.00051209).*

*daf-19(of6)* worms' roaming behavior was different from that of N2 wild-type only once out of the eight assay dates (8/6/2015), the day on which the average grids hit by *daf-19(of6)* worms was oddly lower (*p=0.0001)*. However, it is still significantly different from *daf-19(m86) (p=0.000299)* on that date. Based on the roaming and dwelling behavioral phenotypes displayed (Figure 11), these data suggest that *daf-19(of6)* is not a mutant of DAF-19C and that the mutation in DAF-19B does not significantly affect roaming behavior.

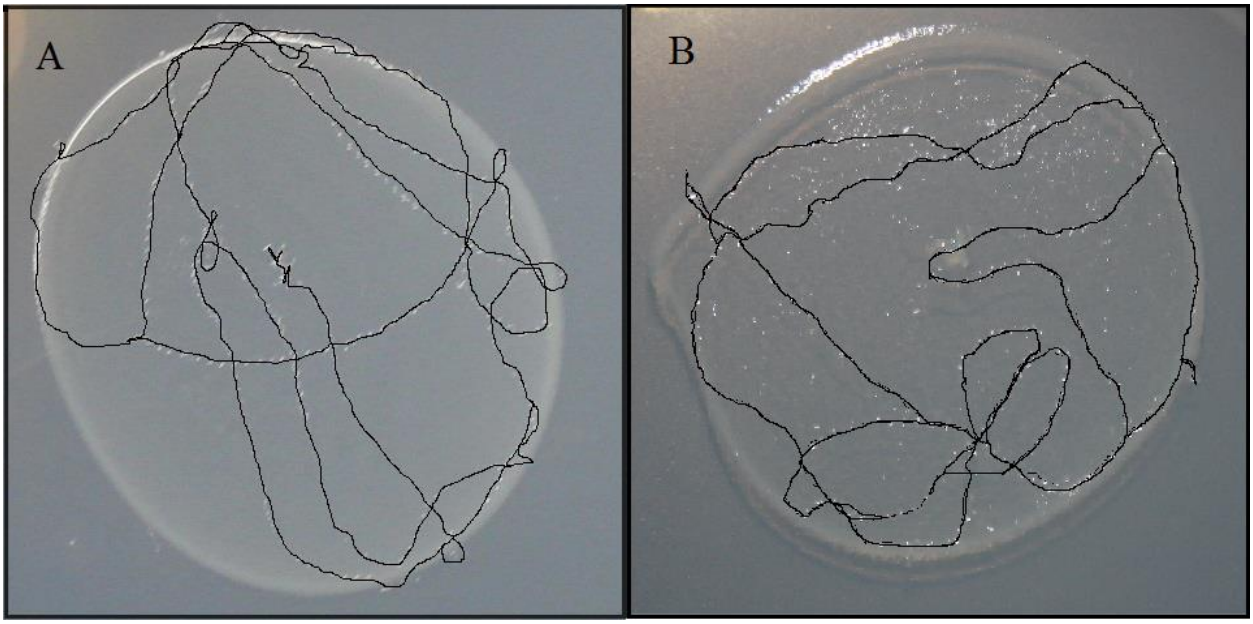


**Figure 11: Dwelling/Roaming Tracks of N2 and *daf-19(of6)* Worms.** Images taken after the assay performed on 1/29/2016. Images zoomed in to only show *E. coli* food area. A) Single N2 worm tracks covering 82% of grids of the food spot. B) Single *daf-19(of6)* worm tracks covering 70% of the food spot.

*daf-19(of5)* worms, on the other hand, displayed highly variable behavior ranging from as little roaming as *daf-19(m86)* to more roaming than N2 wild-type worms. The degree of roaming was significantly different from that of N2 on half of the assay dates (Table 2). Dwelling and roaming behavior observed within assays were variable worm to worm. While some individual worms would roam and behave like N2 wild-type worms, others would roam and dwell slightly more than *daf-19(m86)* worms (Fig.12).

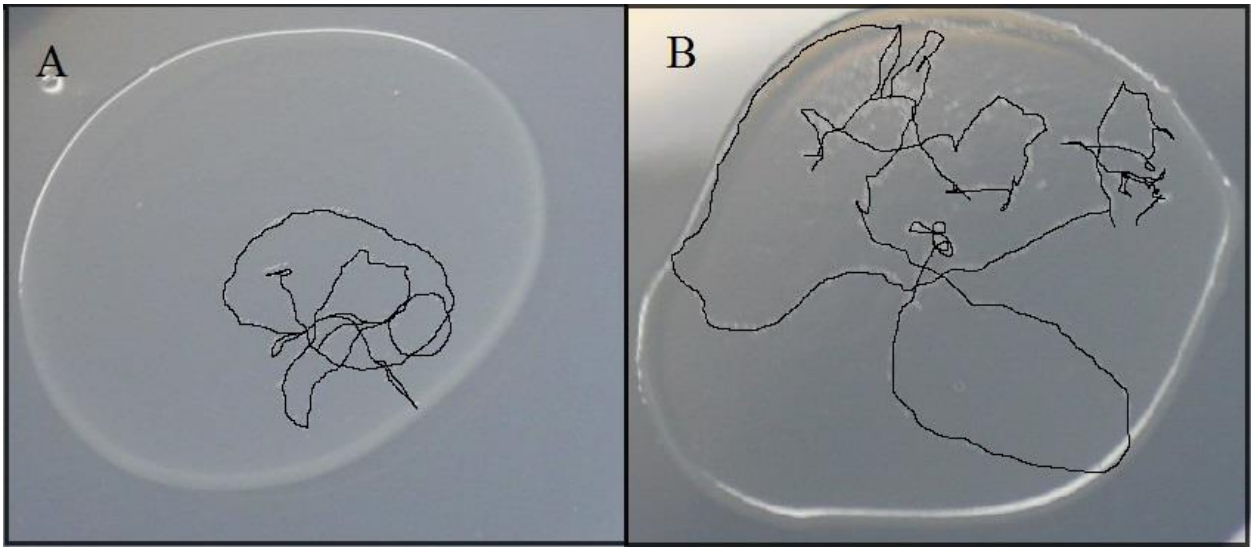


**Figure 12: Dwelling and Roaming Tracks from *daf-19(of5).*** Images taken after the same assay performed on 1/29/2015. A) Single *daf-19(of5)* worm covering 40% of the food lawn. B) Single *daf-19(of5)* worm covering 72% of the food lawn. Both worms were on the assay plate for an hour.

The variability among individual *daf-19(of5)* worms within a single population contributes to the fact that the average percent of total grids crossed ranged from 23% to 77% (Fig. 8). The only date for which *daf-19(of5)* worms roamed that was significantly different from both N2 wild-type and *daf-19(m86)* was on 1/29/2016 (Table 2), when *daf-19(of5)* worms had a higher average degree of roaming than did N2 wild-type worms.

| | N2 | *m86* | Assay Date |
|---|---|---|---|
| *of5* | 0.9633 | 0.000128 | 8/4/2015 |
| *of5* | 2.03E-05 | 0.3456 | 8/6/2015 |
| *of5* | 2.03E-05 | 0.7635 | 8/11/2015 |
| *of5* | 0.997 | 2.03E-05 | 8/18/2015 |
| *of5* | 2.03E-05 | 0.7374 | 8/27/2015 |
| *of5* | 1 | 0.000301 | 1/22/2016 |
| *of5* | 0.02657 | 1.72E-05 | 1/29/2016 |
| *of5* | 0.9982 | 1.72E-05 | 2/5/2016 |

**Table 2: Tukey's Pairwise Comparison between *daf-19(of5)* worms and wild-type and *daf-19* null controls.** P-values are shown from comparison of arcsine transformed frequency of grids hit/total grids containing food. Significant p-values are highlighted in yellow.

*daf-19(tm5562)* worms usually displayed aberrant behavior, however their roaming was not as defective as *daf-19(m86)* worms, nor as variable as *daf-19(of5)* worms. *daf-19(tm5562)* worms roamed to a degree that is significantly different from N2 wild-type (Table 3); seven of eight replicates had a significantly lower average total grids hit than did N2 worms (Fig. 8).

| | N2 | *m86* | Assay Date |
|---|---|---|---|
| *tm5562* | 0.06069 | 0.9537 | 8/4/2015 |
| *tm5562* | 0.000124 | 0.000244 | 8/6/2015 |
| *tm5562* | 2.03E-05 | 0.9998 | 8/11/2015 |
| *tm5562* | 9.64E-05 | 0.003863 | 8/18/2015 |
| *tm5562* | 2.03E-05 | 0.9998 | 8/27/2015 |
| *tm5562* | 0.002262 | 1.72E-05 | 1/22/2016 |
| *tm5562* | 2.68E-05 | 8.22E-05 | 1/29/2016 |
| *tm5562* | 0.005353 | 0.03045 | 2/5/2016 |

**Table 3: Tukey's Pairwise Comparison between *daf-19(tm5562)* worms and wild-type and *daf-19* null controls.** P-values are shown; significant values are highlighted.

Interestingly, in the first replicate on August 4th, wild-type N2 worms roamed less than was typical, giving the Tukey's Pairwise comparison between N2 and *tm5562* a p-value of (0.06). *daf-19(tm5562)* worms also roamed more than did *daf-19(m86)* worms on five of eight dates (Fig. 8).

**Dwelling and roaming: *daf-19a* Rescued Strains**

In order to determine whether the behavioral defects that result from *daf-19* mutations are due to the loss of DAF-19A, three *daf-19a* rescue strains were constructed in *daf-19(of5)*, *daf-19(tm5562)*, *daf-19(m86)* backgrounds. Senti and Swoboda (2008) already showed that adding a *daf-19a* cDNA construct to *daf-19(m86)* mutant worms would only rescue roaming behavior. Therefore, as expected, when we assessed the behavior of *daf-19(m86)* worms expressing the *daf-19a* cDNA, we found that roaming defects were not consistently rescued but were significantly higher than *daf-19(m86)* roaming on one of three dates (Fig. 9).

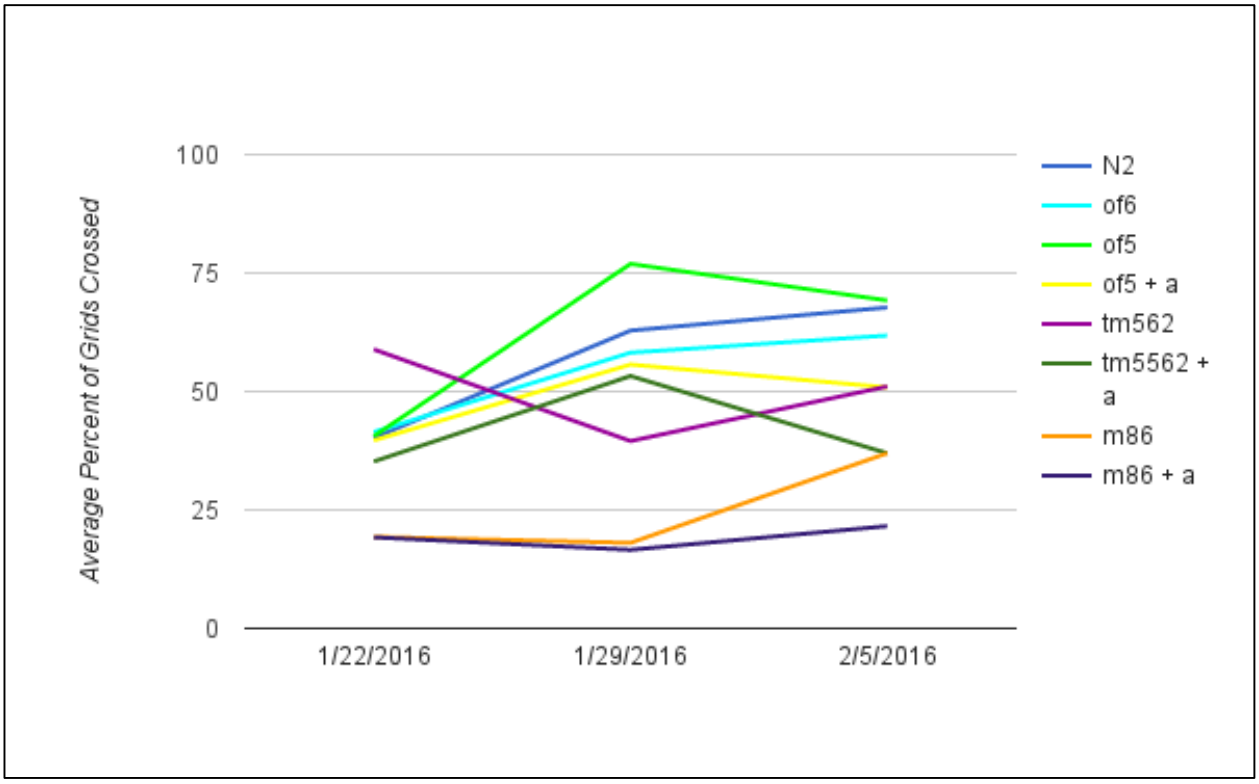


**Figure 13: DAF-19A rescue of roaming behavior is inconsistent.** The average percent of grids crossed per assay date by daf-19 mutant worms and by matched daf-19A rescued strains is shown. Raw data were arcsine transformed in order to improve normality, then back transformed into percentages.

DAF-19A expression does appear to rescue the 'over-roaming' defect of *daf-19(of5)* worms. *daf-19(of5)* worms were significantly rescued by *daf-19a* cDNA addition on 1/29/2016 (*p=0.00047)* and on 2/5/2016 *(p=0.0031)* (Fig. 9). In contrast, *daf-19(of5) +a* was different from N2 on only one of three days (*p=0.00985)*.

From the dwelling and roaming data (Figure 13), *daf-19(tm5562) + a* appears to have a rescued roaming behavior, significantly different from the parent strain on only one of three dates (p=*0.0000544). daf-19(tm5562) + a* was significantly different from N2 only for one of three days *(p=0.0000322)*. This was the date that *daf-19(tm5562) + a* did not roam as much as expected. The other two assay dates *daf-19(tm5562) + a* and N2 wild-type were similar *(p=0.9695, 0.5232)*, raising the average in order to normalize it closer to N2 (Fig 9.). *daf-19(tm5562) + a* was different from *m86* for two of three dates (*p=0.02175, 0.0000322)*. On the third assay date, *daf-19(m86)* had a higher average total grids hit than usual, and *daf-19(tm5562) + a* had a lower average percent, resulting in a p-value of 1.

**Food Foraging: 5-Spot**

In order to further determine the effect of mutant alleles on nervous system function and behavior, we have developed a related assay that mimics a patchy food environment. This assay incorporates the equidistant 5-spot pattern that is seen on dice. Each bacterial food spot diameter is slightly larger than an average one-day old adult worm. Food foraging behavioral tactics were exemplified by the small size of each food spot because a worm that would "roam" would exhaust the immediate food supply and would search for a newer supply of food. Ideally, as seen in wild type behavior, worms that sought out new food would find one or more food spots (apart from the original food spot they were placed on) and dwell. If the wild type worm would not find the new food spot, it would return to the original food spot.

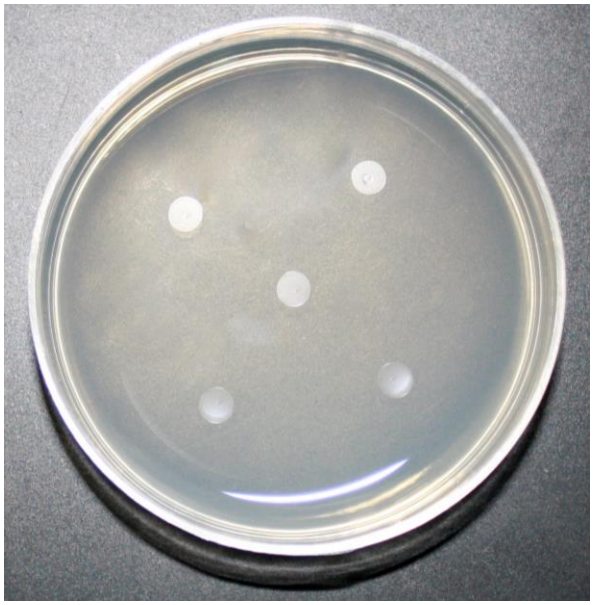

**Figure 14: 5-Spot assay plate.** Every assay plate was pipetted by hand 36-48 hours prior to assay.

In order to further encourage food foraging behavior, food spots were made with a low density food source, (the *E. coli* culture had an absorbance at 600nm of 0.5) to ensure that a virtually nonexistent or very thin OP-50 ring would form. We hoped that excluding the option of dwelling within the outer thicker ring of bacteria would encourage worms to seek out new food if

the nervous system was functional. The lack of bacterial food on the assay plates was a more sensitive way to measure slight behavioral changes in the *daf-19* mutants *of5* and *tm5562.*

The data categories were based on the behavior observed after a single worm was placed in the middle food spot for one hour. Behavior was determined by the location of the worm after one hour on the plate. Worms that were removed from the agar with no trail or path on other food spots were categorized as “left.” Worms that had roamed to find one other food spot either stayed and dwelled at the second food spot, or they kept roaming to find a third food spot or remained foodless in the agar abyss. Other worms “left and returned,” that is, the worm tracks would show that the worm clearly left the original food spot, was on the agar, and returned to the food again. Worms that roamed only within the original food spot for the assay hour were categorized as “never left.”

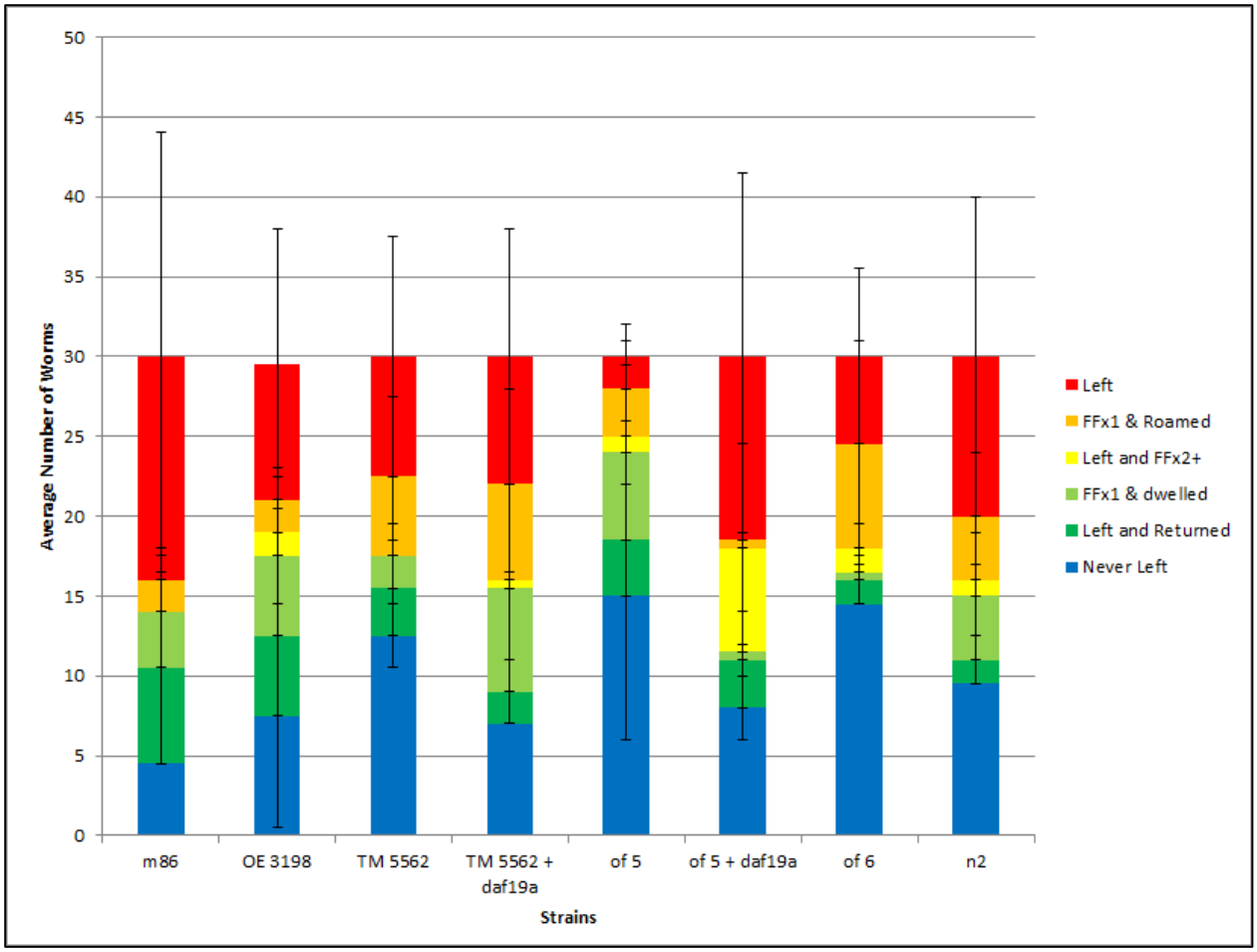


**Figure 15: 5-Spot Behavioral Categories**. Behavior during one hour on the 5-spot agar plate. Average number of worms between two replicates is shown.

Although these results are not discernibly significant with only two replicates, the data illuminate slight behavioral defects displayed by *daf-19* mutants. *daf-19(m86)* worms tend to under-dwell and their behavior is sporadic. Due to the lack of cilia, *daf-19(m86)* worms cannot sense when they have left the original food spot, as N2 wild-type worms can, and when they do roam back into the original spot or to a new food spot, they do not dwell. Most of the time, when a *daf-19(m86)* worm finds a second food spot, the tracks cross the food spot without any sign of dwelling. As seen in the dwelling/roaming assay (Fig. 8), *daf-19(of5)* behavior was variable. In the dwelling/roaming assays, they over-roamed, filling the majority of the large lawn of bacteria. In the 5-Spot assay, they over-dwelled. The addition of *daf-19a* did lower the over-dwelling

behavior in either *daf-19(of5)* or *daf-19(tm5562)* to the N2 wild-type level. The addition of *daf-19a* raised the dwelling behavior in *daf-19(m86)* due to the assay's sensitivity to dwelling in the original food spot. Since the assay is more sensitive to dwelling/roaming behavior, and since the variation between populations of the *daf-19* mutants is so high, the difference between *daf-19(of5)* and *daf-19(tm5562)* and their rescue strains would be better distinguishable with more replications.

We collapsed the six categories into the two broader food foraging behavioral categories of dwelling and roaming (Fig. 15). The overall "dwelling" category consists of "never left," "left and returned," and "found food once and dwelled," while "roaming" consists of "found food twice," "found food once and roamed," and "left." In this manner, we can assess how the 5-Spot compares with the dwelling/roaming assay. In the dwelling/roaming version of the 5-Spot assay, N2 wild-type dwells and roams equally. *daf-19(m86)* over-roams. The addition of *daf-19a* reduced the roaming behavior, and increased the dwelling behavior. *daf-19(of6)* over-dwelled but the discrepancy was not large as *daf-19(of5)* and *daf-19(tm5562)*. Adding *daf-19a* cDNA back to *daf-19(tm5562)* decreased the over-dwelling to almost match with N2 wild-type. Adding *daf-19a* back to *daf-19(of5)* appears to rescue the over-dwelling phenotype and the behavior changed to roaming more than N2 wild-type.

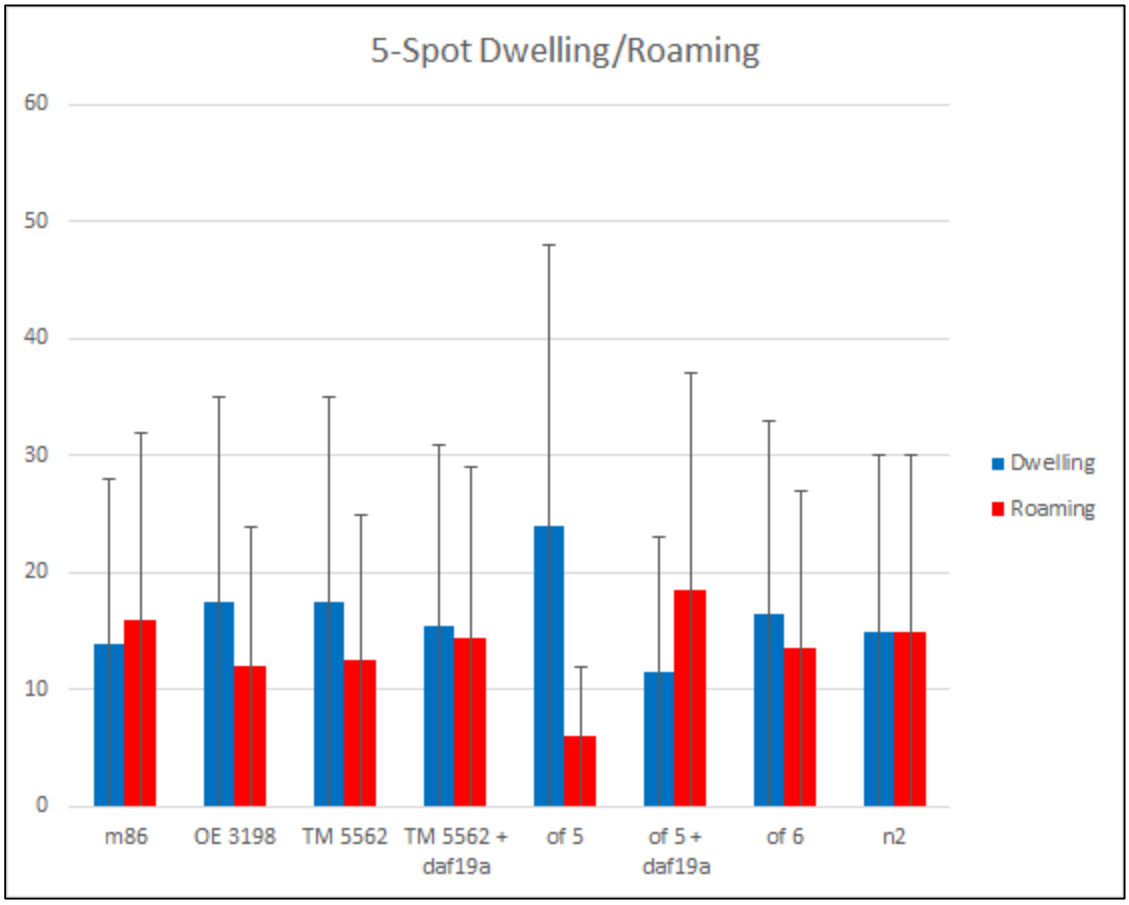


**Figure 16: 5-Spot data collapsed into dwelling/roaming categories.** Two replicates of n=30 per strain.

The dwelling/roaming behavioral phenotypes displayed by the *daf-19* mutants would be better distinguishable from more replicates. The preliminary data from 5-spot assay does suggest that in food foraging conditions, the two *daf-19* mutants over-dwell, whether it is in the original food spot or in the second food spot (Fig. 14). Presumably, since *daf-19(of5)* has functioning cilia, the absence of *DAF-19A* results in over-dwelling.

**Assay of Synaptic Function: Response to Aldicarb**

To assess how the *daf-19* mutations are affecting the function of the neuronal network, we tested the *daf-19* mutants' response to aldicarb. Aldicarb is a pharmacological substance that is an acetylcholine esterase inhibitor, the action of which leads to the accumulation of acetylcholine in the synaptic cleft. The increase acetylcholine in the synaptic connections tells muscles to contract until the cleft is over-stimulated and the stimulation results in paralysis. Senti and Swoboda (2008) showed that *daf-19* mutants (such as *daf-19(m86))* displayed moderate, but significant, resistance to aldicarb compared to N2 wild-type worms. In our assay, *daf-19(m86)* was as resistant as the control, *unc-29(e1072),* worms to aldicarb. This resistance could be the result of a pre-synaptic or post-synaptic neuronal defect. N2 wild-type worms were the least resistant (most sensitive) to aldicarb. *daf-19(of5)* was the second most sensitive strain (slope=-2.7515), most similar to the N2 wild-type worms, showing us that the presumably functional cilia produced by DAF-19C are in fact functional, therefore resulting in sensitivity to aldicarb. *daf-19(tm5562)* worms were not as sensitive to aldicarb as were *daf-19(of5)* worms (slope=-2.5273), but were less resistant than *daf-19(m86)* and *unc-29(e1072)* worms (Fig. 16).

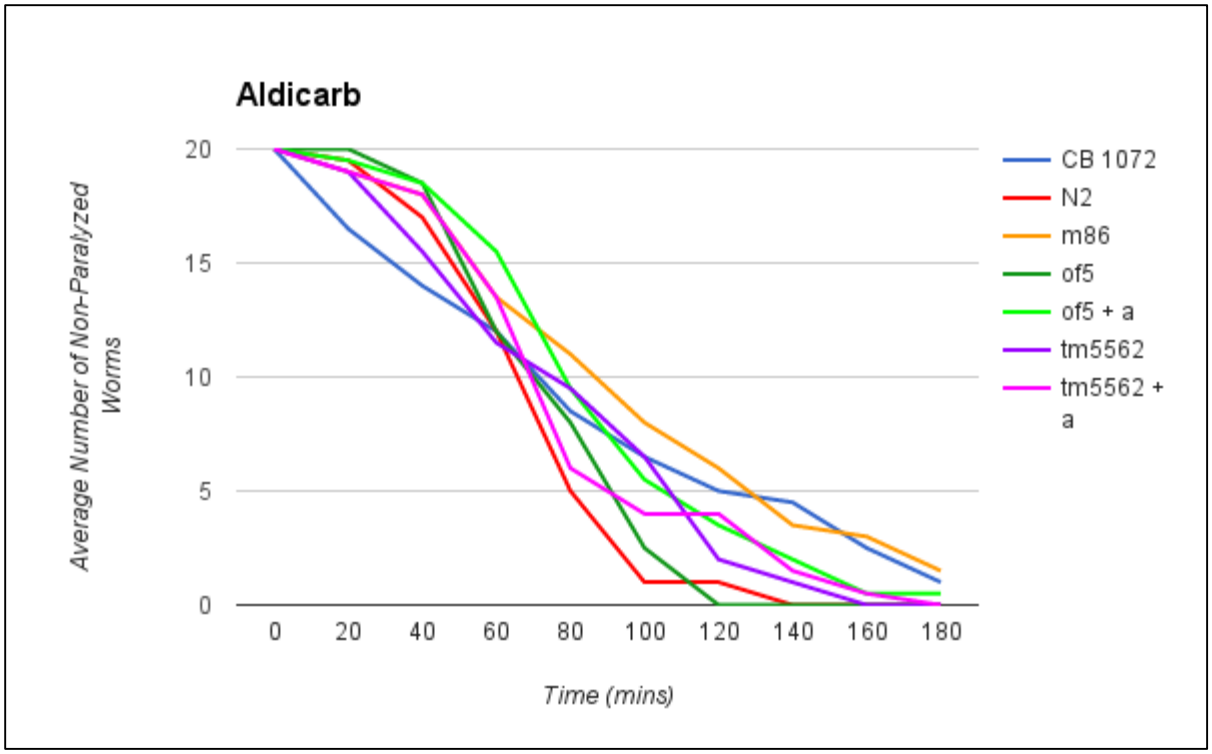


**Figure 17: Response to Aldicarb.** The number of worms still moving after exposure to aldicarb for the indicated number of minutes. Worms were proclaimed as "paralyzed" after being prodded on the head three times without significant bodily movements, then removed from the assay plate. Worms were prodded every 20 minutes. Two replications of n=20 each.

| Strain | Average Rate of Paralysis |
|---|---|
| **unc-29** | -2.0576 |
| **N2** | -2.6576 |
| **m86** | -2.28165 |
| **of5** | -2.7515 |
| **of5+a** | -2.6121 |
| **tm5562** | -2.5273 |
| **tm5562+a** | -2.55605 |

**Table 3: Average Rate of Paralysis per Strain.**

The addition of *daf-19a* does slightly increase resistance to aldicarb compared to parent strains *daf-19(tm5562)* and *daf-19(of5).* It increases the rate of paralysis of *daf-19(of5)* from a slope of -2.7515 to a slope of -2.6121. Both of the *daf-19a* rescue strains are more resistant to aldicarb for a longer period of time than their *daf-19* mutant counterparts (Fig. 16). They both lasted longer than *daf-19(tm5562)* and *daf-19(of5)* but are not as resistant as *daf-19(m86)* or *unc-29(e1072)* worms.

To further explore resistance to aldicarb, we found the average slope or rate of paralysis from minutes 60-100 for the two replicates. It was at the time in the assay that N2 wild-type, the most sensitive to aldicarb quickly resulting in zero worms resistant the pharmacological substance. We wanted to see what the rate of paralysis was for our *daf-19* mutants when our control worm population were beginning to be completely paralyzed.

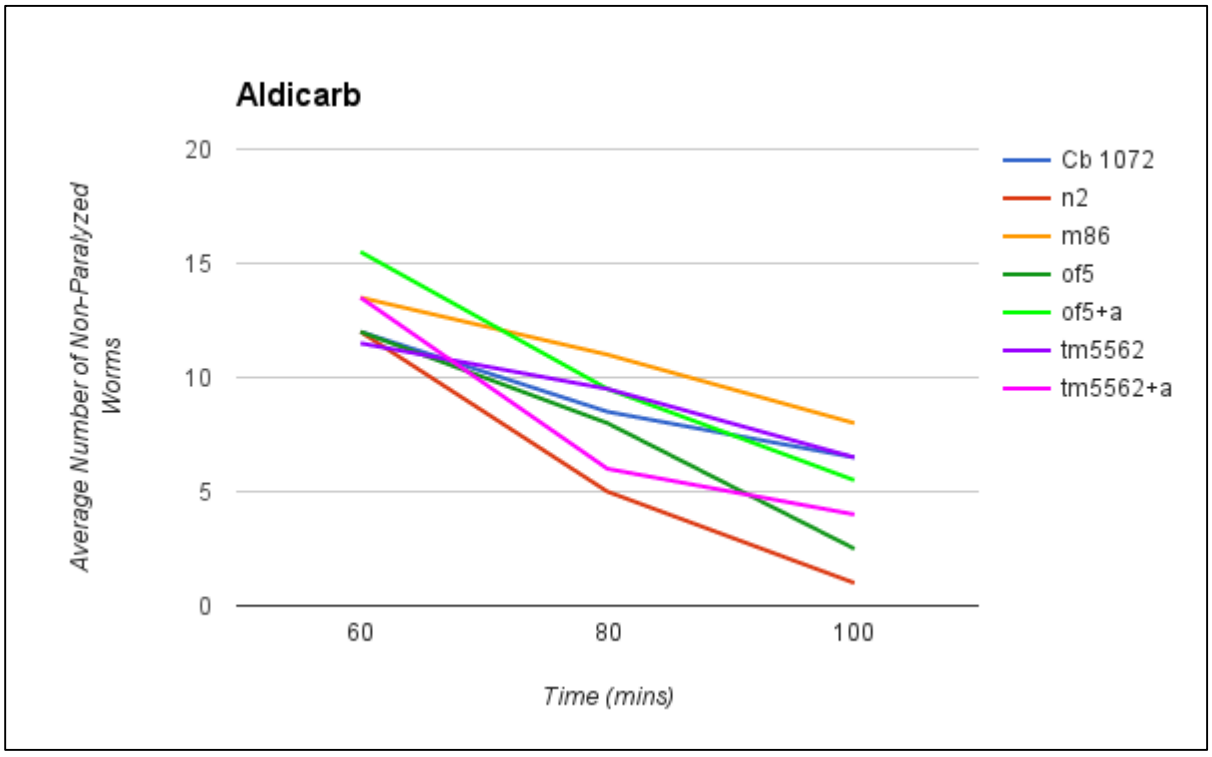


**Figure 18: Response to Aldicarb.** The number of worms still moving after exposure to aldicarb for the indicated number of minutes. Worms were proclaimed as "paralyzed" after being prodded on the head three times without significant bodily movements, then removed from the assay plate. Worms were prodded every 20 minutes. Two replications of n=20 each. Graph focused in from Figure 16 to emphasize slopes of resistance to aldicarb.

| Strain | Average rate of paralysis |
|---|---|
| **unc-29** | -2.75 |
| **N2** | -5.5 |
| **m86** | -2.75 |
| **of5** | -4.75 |
| **of5+a** | -5 |
| **tm5562** | -2.5 |
| **tm5562+a** | -4.75 |

**Table 4: Average Rate of Paralysis Minutes 60-100 of Aldicarb Assay.**

*daf-19(m86)* and *unc*-29 worms are the most resistant during minutes 60-100 with the same slope of -2.75. N2 wild-type has the steepest rate of paralysis of -5.5 demonstrating its sensitivity (non-resistance) to aldicarb due to its functional cilia. *daf-19(of5)* worms were paralyzed less quickly (slope of -4.75) while adding back *daf-19a* increases their sensitivity to aldicarb to that of wild type levels (slope = -5). The biggest change in aldicarb resistance was the change seen in *daf-19(tm5562)* worms and *daf-19(tm5562) + a* worms in which *daf-19a* cDNA is expressed. In this case, the slope representing paralysis rate changed from from -2.5 to -4.75 (Table 4). The addition of *daf-19a*, which was thought to be involved with synaptic function and maintenance with DAF-19B, improved the sensitivity of the response to aldicarb to that of N2 wild-type worms. This dramatic change demonstrates that DAF-19A does improve synaptic function of neurons in *daf-19(of5)* worms.

In order to determine if the mutations in *daf-19* affect the pre- or post-synaptic cleft, more replications must be done to test resistance against both aldicarb and levamisole. Aldicarb resistance shows that the mutation could have an effect on presynaptic or post-synaptic neurons while a resistance to levamisole, an acetylcholine receptor agonist, will show if the defect is post-synaptic because it activates cholinergic receptors independent of presynaptic input. Since *daf-19(of5)* has such variable dwelling roaming behavior (Fig. 11), and it was sensitive to aldicarb, it may be that the mutation affects the presynaptic neuron. More replications for resistance to aldicarb are needed to further examine the neuronal deficiencies that our *daf-19*

mutants show, as well as multiple replicates of an assay demonstrating the response to levamisole.

## Discussion

Senti and Swoboda (2008) found that different DAF-19 isoforms have distinct functions in subsets of neurons. The DAF-19C isoform of this transcription factor is known to regulate the expression of genes that are required for the structure and function of cilia in *C. elegans*, while some data suggest that DAF-19A/B regulates synaptic protein/vesicle maintenance. Previous work also demonstrated that all DAF-19 isoforms were necessary for fully wild-type dwelling and roaming behavior. We seek to further understand the function of DAF-19 isoforms in neuronal processes other than ciliogenesis. We believe that characterizing the behavioral defects of new *daf-19* mutations, which affect specific *daf-19* isoforms, will lead us to understand whether neuronal functions require the activity of other DAF-19 isoforms.

### Isoform Specificity of New *daf-19* Mutant Alleles

The *daf-19(of6)* worms are mutated in order that presumably DAF-19B and C are affected, leaving DAF-19A intact. However, *daf-19(of6)* worms dye-fill, and are not dauer-constitutive and, in our assay do not have any apparent behavioral phenotypes that differentiate them from N2 wild-type worms. These data suggest that only DAF-19B is being affected, because exon 4 is not in DAF-19A due to differential splicing.

The *daf-19(of5)* worms contain a mutation predicted to affect DAF-19A&B, however since *daf-19(of6)* worms have no apparent defects, we can presume that DAF-19B has no

apparent neuronal role in the *C. elegans* nervous system. We therefore conclude that *daf-19(of5)* worms will illustrate the effects of a mutation to be DAF-19A.

The *daf-19(tm5562)* mutation is also predicted to affect DAF-19A&B, by deleting exon 2 which is only expressed in these longer DAF-19 isoforms. It is possible that this mutation might also affect the expression of DAF-19C through the deletion of intron sequences flanking exon 2, if the intron deletion affects the control region for *daf-19C* transcription. This hypothesis has not been directly tested and our data do not, in fact, support an effect on DAF-19C expression.

**Behavioral and Neuronal Functions of DAF-19 Isoforms**

We used a dwelling/roaming assay to quantify defective behavioral phenotypes observed of *daf-19* mutants by determining track coverage on an OP-50 food spot. *daf-19(of6)* worms behaved differently from N2 worms only once out of the eight assay dates, and, like N2 worms, undertook significantly more roaming than did *daf-19(m86)* worms. This conclusion holds true for both assays in which the behavior of *daf-19(of6)* worms were assessed. We therefore conclude that the mutation in *daf-19(of6)* worms does not affect an isoform that contributes significantly to the behaviors assayed here. *daf-19(of6)* worms properly dye-fill and are not dauer-constitute, thus we assume that DAF-19C is produced and is functional. Our behavioral data provide further support for this conclusion. A positive dye-filling assay proves that there is ciliary structure in the neurons of a worm. The similarity in dwelling/roaming behavior to N2 wild-type suggests that *daf-19(of6)* ciliary structure has normal function as well. These two phenotypes displayed by *daf-19(of6)* suggest that it is not a mutant of DAF-19C. The *of6* mutation should eliminate functional DAF-19B as well. Again, since this mutant allele does not

significantly affect roaming/dwelling behavior, we can conclude that DAF-19B does not play a role in the neuronal functions required for dwelling and roaming behavior. We chose to not test *daf-19(of6)* worms against aldicarb because they behave like N2 wild-type, thus there is no indication of aberrant neuronal function.

*daf-19(of5)* worms also have proper dye-filling neurons, thus they have properly structured and functional cilia and we can presume that DAF-19C is unaffected. However, the highly variable defective roaming behavior observed in *daf-19(of5)* worms suggests that DAF-19A/B is responsible for the inconsistencies in behavior. Since we have already eliminated a role for DAF-19B, based on the normal behavior of *daf-19(of6)* worms, we can conclude that any aberrant behaviors of *daf-19(of5)* animals are due to the loss of DAF-19A. For the most part, *daf-19(of5)* worms over-roamed in the dwelling/roaming assay and adding back *daf-19a* cDNA appeared to lower the over-roaming phenotype to match that of the N2 wild-type worms. Oddly, addition of *daf-19a* made the *daf-19(of5)* worms slightly more resistant to aldicarb. The *daf-19(of5)* worms over-dwelling in the 5-Spot assaying, which led us to assume that the absence of *DAF-19A* results in worms staying within an area of food and fully exploring that area of food – whatever the size of the food patch – but not leaving the food patch in search of new food. These data suggest that the absence of *daf-19a* negatively affects neuronal structure or function. The higher variability in behavioral phenotypes observed in this strain is most likely the result of variable gene expression, worm-to-worm. It is possible that the mutation affects DAF-19A expression. This hypothesis would need to be tested by assessments of DAF-19A protein levels using antibodies specific to the N-terminus of the long isoform.

*daf-19(tm5562)* worms are missing exon 2, and the DAF-19A/B isoforms are expected to be affected. As above, we can eliminate effects of DAF-19B reduction based on the behavior of

*daf-19(of6)* worms, leaving this allele to, again, affect only DAF-19A production. The dwelling/roaming behavior of *daf-19(tm5562)* worms is not as aberrant as that of *daf-19(m86)* worms nor as variable as *daf-19(of5)* worms, however the addition of *daf-19a* does rescue the sensitivity to aldicarb, increasing the rate of paralysis to behave like N2 wild-type (Table 4). In the 5-spot assay, the addition of *daf-19a* lowers the over-dwelling phenotype observed in *daf-19(tm5562)* mutants.

Both DAF-19A mutants are also not completely resistant to aldicarb as are *daf-19(m86)* worms, but they are somewhat more resistant to this drug than are wild type worms. In both strains, addition of daf-a cDNA restores wild type levels of aldicarb sensitivity. These results suggest that *daf-19a* is solely responsible for the synaptic defects that underlie aldicarb sensitivity.

**Future Directions**

To further establish the role of DAF-19A&B in behavioral and neuronal function, it would be interesting to test our *daf-19* mutants against levamisole. If the addition *daf-19a* could also rescue sensitivity to the *daf-19* mutants, we could positively say that DAF-19B has no apparent role in neuronal connectivity.

The deletion of *daf-19a* in *daf-19(tm5562)* increased aldicarb resistance, demonstrating again that *daf-19a* is necessary for synaptic function, and that *daf-19(tm5562)* is a true DAF-19A mutant. It was believed that *daf-19(of5)* was also a DAF-19A mutant, but its highly variable results in dwelling/roaming behavior suggests that there may be an offsite target that is linked to chromosome 2 that affects the variability of DAF-19A expression in *daf-19(of5).* It may be that it

is not completely back-crossed and there are other mutations affecting the variable expression that we have observed. It is imperative to test a correct *daf-19(of5)* mutation against *daf-19(tm5562)* to see how mutations in exon 1 and 2 affect the expression of DAF-19A.

Other factors that may contribute to variability are the rate at which the *daf-19* mutants age. Even though all worms are picked at the same life stage previous to the assay, they may not all be at the same developmental stage when the assay is preformed, accounting for variability in *daf-19* protein produced that affects behavior. More replicates of the 5-Spot assay should be preformed to further examine how *daf-19*a affects the sensation of food while roaming.

**Acknowledgements**

I would like to acknowledge and thank Professor De Stasio for the opportunity to work in her lab and for guiding me through the honors thesis process. I would like to thank all the members in the De Stasio lab for being such a wonderful, collaborative group. I would also love to thank Wayne Krueger and JoAnn Stamm in the stock room, this research could not have happened without their patience and help. I would also like to thank Rachel Crowl for providing images of assay plates. Finally, to my friends and family that have supported me throughout my undergraduate career.

**Literature Cited**

Aftab S, Semenec L, Chu JS, Chen N (2008)."Identification and characterization of novel human tissue-specific RFX transcription factors". *BMC Evol. Biol.* **8**: 226. doi:10.1186/1471-2148-8-226.PMC 2533330. PMID 18673564.

Altun, Z.F. and Hall, D.H. 2009. Introduction. In *WormAtlas* .doi:10.3908/wormatlas.1.1

Altun, Z.F. and Hall, D.H. 2011. Nervous system, general description. In *WormAtlas*. doi:10.3908/wormatlas.1.18

Berg JM, Tymoczko JL, Stryer L. Biochemistry. 5th edition. New York: W H Freeman; 2002. Chapter 3, Protein Structure and Function. Available from: http://www.ncbi.nlm.nih.gov/books/NBK21177/

Boulin, Thomas. "The Nervous System." *The Mind of the Worm*. WormAtlas, 2001. Web. 26 Feb. 2016.

Chalfie, Martin, John E. Sulston, and Sydney Brenner. "The Neural Circuit for Touch Sensitivity in Caenorhabditis Elegans." *The Journal of Neuroscience* (1985): 956-64. Print.

Chalfie, M.; et al. (1994). "Green fluorescent protein as a marker for gene expression". *Science* 263(5148): 802–805. doi:10.1126/science.8303295.PMID 8303295.

Chklovskii, Dmitri B., and Cornelia I. Bargmann. "The Mind of a Male?" *Sciencemag.org*. Science, 27 July 2012. Web. 21 Feb. 2016.

Chu, Jeffery S. C. et al. "Fine Tuning of RFX/DAF-19-Regulated Target Gene Expression through Binding to Multiple Sites in *Caenorhabditis Elegans*." *Nucleic Acids Research* 40.1 (2012): 53–64. *PMC*. Web.

Dimitriadi, Maria, and Anne C. Hart. "Neurodegenerative Disorders: Insights from the Nematode *Caenorhabditis Elegans*." *Neurobiology of disease* 40.1 (2010): 4–11. *PMC*. Web. 5 Mar. 2016.

Dubruille, R., A. Laurencon, E. Shishido, M. Coulon-Bublex, P. Swoboda, P. Couble, M. Kernan, and Durand B. "Drosophila Regulatory Factor X Is Necessary for Ciliated Sensory Neuron Differentiation." *National Center for Biotechnology Information*. U.S. National Library of Medicine, Dec. 2002. Web. 10 Nov. 2015.

Falk, Nathalie et al. "Specialized Cilia in Mammalian Sensory Systems." Ed. Gang Dong and William Tsang. *Cells* 4.3 (2015): 500–519. *PMC*. Web. 28 Jan. 2016.

"Genes and Mapped Phenotypes." *National Center for Biotechnology Information*. U.S. National Library of Medicine, n.d. Web. 14 Feb. 2016.

Gilliam, Jared C. et al. "Three-Dimensional Architecture of the Rod Sensory Cilium and Its Disruption in Retinal Neurodegeneration." *Cell* 151.5 (2012): 1029–1041. *PMC*. Web. 14 Feb. 2016.

Hart, A.C., Sims, S., and Kaplan, J.M. (1995). Synaptic code for sensory modalities revealed by *C. elegans* GLR-1 glutamate receptor. Nature *378*, 82–85.

Hart, Anne C., ed. Behavior (July 3, 2006), *WormBook*, ed. The *C. elegans* Research Community, WormBook, doi/10.1895/wormbook.1.87.1, http://www.wormbook.org.

Hutter, Herald. "C. Elegans Nervous System." *C. Elegans Nervous System*. Simon Fraser University, 12 Jan. 2008. Web.

Inglis PN, Ou G, Leroux MR, et al. (2007) The sensory cilia of Caenorhabditis elegans. In: WormBook: The Online Review of C. elegans Biology [Internet]. Pasadena (CA): WormBook; 2005-. Available from: http://www.ncbi.nlm.nih.gov/books/NBK19729/

Kaplan, J M, and H R Horvitz. "A Dual Mechanosensory and Chemosensory Neuron in Caenorhabditis Elegans." *Proceedings of the National Academy of Sciences of the United States of America* 90.6 (1993): 2227–2231. Print.

Konnikova, Maria. "The Power of Touch." *The New Yorker*. The New Yorker, 04 Mar. 2015. Web. 27 Jan. 2016.

Lints, R. and Hall, D.H. 2005. Handbook of *C. elegans* Male Anatomy. In *WormAtlas*. http://www.wormatlas.org/male/malehomepage.htm

Lints, R. and Hall, D.H. 2009. Male reproductive system, general description. In *WormAtlas*. doi:10.3908/wormatlas.2.14 Edited for the web by Laura A. Herndon. Last revision: July 22, 2013.

Liu, Jeh-Ping, and Scott O. Zeitlin. "The Long and the Short of Aberrant Ciliogenesis in Huntington Disease." *The Journal of Clinical Investigation*121.11 (2011): 4237–4241. *PMC*. Web. 21 Feb. 2016.

Lodish H, Berk A, Zipursky SL, et al. Molecular Cell Biology. 4th edition. New York: W. H. Freeman; 2000. Section 21.1, Overview of Neuron Structure and Function. Available from: http://www.ncbi.nlm.nih.gov/books/NBK21535/

Mahoney, T. R., S. Luo, and M. L. Nonet. "Analysis of Synaptic Transmission in Caenorhabditis Elegans Using an Aldicarb-sensitivity Assay." *NCBI*. National Center for Biotechnology Information,, 2006. Web. 25 Feb. 2016.

Mitreva, Makedonka. "Genome: Caenorhabditis Elegans." *Genome*. 2014 Washington University in St. Louis, n.d. Web. 08 Feb. 2016.

Purves, Dale. "The Olfactory Epithelium and Olfactory Receptor Neurons." *The Olfactory Epithelium and Olfactory Receptor Neurons*. U.S. National Library of Medicine, 2001. Web. 28 Jan. 2016.

Qian, Hai et al. "Levamisole Resistance Resolved at the Single-Channel Level in *Caenorhabditis Elegans*." *The FASEB Journal* 22.9 (2008): 3247–3254.*PMC*. Web. 26 Feb. 2016.

Raizen, David M., John E. Zimmerman, Matthew H. Maycock, Uyen D. Ta, Young-jai You, Meera V. Sundaram, and Allan I. Pack. "Lethargus Is a Caenorhabditis Elegans Sleep-like State." *Nature*. Nature Publishing Group, 31 Jan. 2008. Web. 10 Feb. 2016.

Sarafoleanu, C., C. Mella, M. Georgescu, and C. Perederco. "The Importance of the Olfactory Sense in the Human Behavior and Evolution." *Journal of Medicine and Life*. Carol Davila University Press, 25 Apr. 2009. Web. 28 Jan. 2016.

Senti, G., and P. Swoboda. "Distinct Isoforms of the RFX Transcription Factor DAF-19 Regulate Ciliogenesis and Maintenance of Synaptic Activity." *Molecular Biology of the Cell* 19.12 (2008): 5517-528. Web.

Swoboda, P., Adler, H. T., & Thomas, J. H. (2000). The RFX-type transcription factor DAF-19 regulates sensory neuron cilium formation in C. elegans. *Mol Cell, 5*, 411-21.

Wang, Juan. , Schwartz, Hillel T., Barr, Maureen M. (2010). Functional Specialization of Sensory Cilia by an RFX Transcription Factor Isoform. GENETICS *December 1, 2010 vol. 186 no. 4, 1295-1307*

Wolkow, C.A. and Hall, D.H. 2016. Handbook of *C. elegans* Dauer Anatomy. In *WormAtlas*.http://www.wormatlas.org/dauer/dauerhomepage.htm